Title

Role of film stoichiometry and interface quality in the performance of (Ba,Sr)TiO3 tunable capacitors with high figures of merit

Journal

Applied Physics Letters, 109(19)

ISSN

0003-6951 1077-3118

Authors

Freeze, Christopher R
Stemmer, Susanne

Publication Date

2016-11-07

DOI

10.1063/1.4967374

Peer reviewed

AIP | Applied Physics Letters

Role of film stoichiometry and interface quality in the performance of (Ba,Sr)TiO3 tunable capacitors with high figures of merit

Christopher R. Freeze and Susanne Stemmer

Citation: Applied Physics Letters **109**, 192904 (2016); doi: 10.1063/1.4967374
View online: http://dx.doi.org/10.1063/1.4967374
View Table of Contents: http://scitation.aip.org/content/aip/journal/apl/109/19?ver=pdfcov
Published by the AIP Publishing

Role of film stoichiometry and interface quality in the performance of (Ba,Sr)TiO_3 tunable capacitors with high figures of merit

Christopher R. Freeze and Susanne Stemmer[a)]
Materials Department, University of California, Santa Barbara, California 93106-5050, USA

(Received 5 August 2016; accepted 26 October 2016; published online 8 November 2016)

Parallel plate capacitors with quality factors exceeding 1000 were fabricated using $Ba_{0.3}Sr_{0.7}TiO_3$ (BST) thin films grown by hybrid molecular beam epitaxy on epitaxial Pt bottom electrodes. The influence of film stoichiometry was investigated by varying the (Ba + Sr)/Ti ratio around the stoichiometric composition. The quality factor is highest for stoichiometric films, but (Ba + Sr)-rich films can be biased to higher fields. Furthermore, two different processes were used to deposit the top electrodes of the parallel plate capacitors. While the quality of the top contact/BST interface did not strongly affect the device quality factor, an enhancement in the dielectric tunability was seen for capacitors with top electrodes deposited at high temperatures, which effectively removes interfacial contamination layers. *Published by AIP Publishing.*
[http://dx.doi.org/10.1063/1.4967374]

Tunable dielectrics, in particular, the perovskite $Ba_xSr_{1-x}TiO_3$ (BST), are actively investigated for microwave circuit applications, such as varactors and resonators.[1–5] A main focus of materials and device optimization is to simultaneously achieve high quality factors ($Q = 1/\tan\delta$, where $\tan\delta$ represents the dielectric loss tangent) while tuning the capacitance at least by a factor of two with an applied DC bias.[2,6] Q-factors exceeding 1000 and tunabilities up to 5:1 were reported in BST films that were grown by molecular beam epitaxy (MBE).[7] Further improving the performance requires understanding of the effects of key materials parameters on tunable device properties. For example, the hybrid MBE approach employed in Ref. 7 is known to result in a very high degree of film stoichiometry[8,9] and a low concentration of point defects.[10,11] Literature data of BST deposited by methods such as sputtering and pulsed laser deposition exhibit a great degree of variability (sometimes by orders of magnitude) in the reported dielectric properties (see, e.g., Table I in Ref. 6). It is thus important to determine the degree to which film stoichiometry affects the tunable device properties. Furthermore, previous studies indicate that a certain degree of BST film non-stoichiometry may benefit other important device parameters, such as leakage.[12] The excellent control over film composition afforded by hybrid MBE makes BST films grown by this method suitable for investigating the role of stoichiometry in tunable device properties.

A second key parameter determining the device properties is the presence of series-connected, low-permittivity layers between the BST and the electrodes.[12] While the origin of these layers was poorly understood for some time,[12] it is now clear that they are primarily contamination layers due to the strong propensity of BST and related materials to adsorb carbon-containing species when exposed to air.[13,14] They can be minimized by using high-temperature processes prior to and during electrode deposition.[14] Less well understood, however, is whether they also affect the dielectric losses, for example, via interface states,[15] in addition to lowering the overall capacitance and tunability. In this Letter, we investigate the role of BST stoichiometry and of interface layers in controlling the dielectric properties of BST parallel-plate capacitors.

Epitaxial Pt bottom electrodes, 100-nm-thick, were grown on (001) $SrTiO_3$ single crystals by DC sputtering, as described elsewhere,[16] and annealed at 1000 °C for 10 min in oxygen. BST films were grown by hybrid molecular beam epitaxy, described previously.[7,17] The hybrid MBE process uses a metal-organic source, titanium tetra isopropoxide (TTIP) to supply Ti and O, whereas Ba and Sr are supplied from effusion cells. Additional oxygen is supplied from an oxygen plasma source. At sufficiently high growth temperatures, the volatile TTIP source allows for a growth window[8] and for very precise stoichiometry control.[9] The substrate temperature was 775 °C (thermocouple read-out) and limited by the need to maintain the (001)-orientation of the Pt, which has a tendency to switch to (111). BST films (280 nm) were grown on Pt electrodes (thickness determined by x-ray reflectivity) with varying TTIP beam equivalent pressures (fluxes) to yield TTIP/(Sr + Ba) flux ratios of 28, 32, 36, 40, and 44. Like $SrTiO_3$[8,18] and $BaTiO_3$,[19] BST films exhibit a minimum in the out-of-plane lattice parameter when the films are cation stoichiometric, that is, have a 1:1 A- to B-site ratio, where $A = Ba + Sr$ and $B = Ti$. Lattice parameters were determined using high-resolution 2θ-ω scans of the 002 BST reflections of films grown on $SrTiO_3$. Within the range of TTIP/(Sr + Ba) flux ratios that yield 1:1 A:B site ratios according to x-ray lattice parameter measurements, a 4×4 surface reconstruction is observed in *in-situ* reflection high-energy electron diffraction (RHEED). This reconstruction indicates A:B site stoichiometry.[9] Flux ratios of 32, 36, and 40 yielded cation stoichiometric films on $SrTiO_3$ by these two measures. Films on platinized $SrTiO_3$ were fully relaxed. Off-axis x-ray scans of the 103 reflections were used to obtain in- and out-of-plane lattice constants,[20] which determined the $Ba_xSr_{1-x}TiO_3$ composition of $x = 0.3$ by comparison with the bulk lattice parameters. Contrary to the 30 min growths on $SrTiO_3$ substrates under the same condition, no

[a)]Author to whom correspondence should be addressed. Electronic mail: stemmer@mrl.ucsb.edu

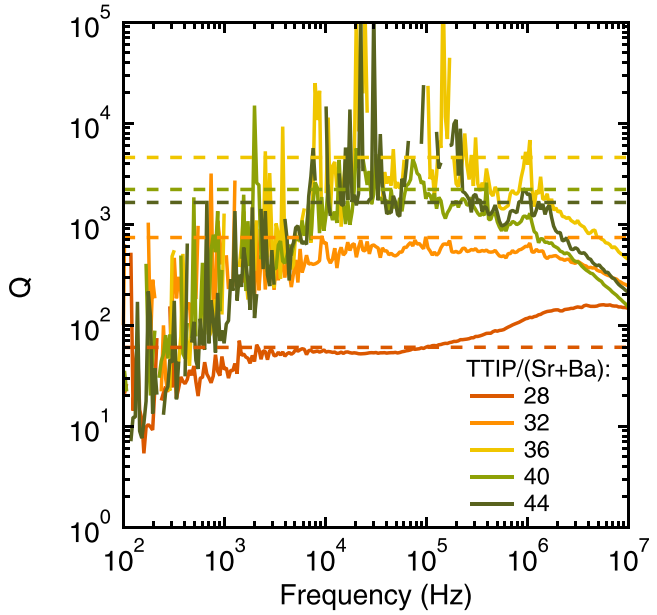

FIG. 1. Quality factor as a function of frequency for devices with sputtered top contacts. The measured data is shown as a solid line, while the dotted line shows Q calculated from fits of $C(f)$.

lattice expansion was observed for off-stoichiometric growths, although RHEED showed clear differences (supplementary material). For growths on platinized $SrTiO_3$, which were used to fabricate devices, only flux ratios of 36 and 40 were stoichiometric by RHEED. BST surfaces were also investigated by atomic force microscopy (AFM) (supplementary material). To fabricate capacitors, 100 nm Pt top electrodes were deposited via either sputtering at 825 °C in 10 mTorr Ar following a 2 h annealing in O_2 or by electron (e)-beam evaporation. Using a two-step mask process, top-contact patterns were etched by Ar ion milling, followed by a mesa etch with the Ar ion mill. After over-etching the active mesa in the ion mill, 80 nm Pt was deposited by e-beam evaporation to thicken exposed areas of the back contact through a liftoff process. Devices were annealed for 20 min at 800 °C in O_2 to minimize any oxygen vacancies. Impedance measurements were taken on an Agilent 4294 A impedance analyzer with picoprobe ground-signal-ground (GSG) probes with 100 μm pitch on $45 \times 45\ \mu m^2$ capacitors with a $60 \times 60\ \mu m^2$ mesa. The AC probe amplitude was 50 mV. For bias sweeps, 50 mV steps and downward sweeps were used.

Figure 1 shows the zero-bias Q as a function of frequency for the capacitors with hot-sputtered Pt, which shows the typical behavior of being dominated by leakage at low frequencies and the series resistance roll-off at high frequencies.[1] In the intermediate range (10^4–10^6 Hz), Q is representative of the intrinsic BST materials Q. The very large Qs of the MBE BST films, exceeding several thousands, approach the accuracy limits of the impedance analyzer. To independently confirm the high Q, a power-law fit to the frequency dependence of the capacitance (C) can be used to estimate Q, as described in Ref. 21. The results, which show good agreement with the Q-measurements, are shown as dashed lines in Fig. 1. The zero-field Q is highest for stoichiometric films (ratios of 36 and 40) and it decreases most strongly for A-site-excess films.

Figure 2 shows the dependence of Q on bias (V), measured at 1 MHz, for the two types of top electrodes. Either a drop or an increase in Q is observed at low V. In particular, the high-Q, stoichiometric BST samples show a decrease in Q, whereas the A-site-rich samples (ratios 28 and 32) show an increase. The latter also showed inconsistency between devices on each sample, and the bias range over which the Q rises varied significantly. For instance, some devices with a flux ratio of 32 and sputtered contacts showed the sharp rise in Q below 0.1 MV/cm, with a continued gradual rise until 0.4–0.5 MV/cm. The origins of the two types of behaviors have been discussed previously.[2] In particular, losses due to many extrinsic mechanisms, such as defects or local polar regions, scale with the permittivity, which decreases with V, causing an increase in Q with V.[2] In contrast, intrinsic losses can cause an increase in loss with bias. For example, quasi-Debye loss appears when the applied voltage breaks the centrosymmetry of the cubic BST unit cell.[2,22] The results in Fig. 2 show that there is a change in the mechanism towards more intrinsic loss mechanisms controlling Q for the stoichiometric compared to the non-stoichiometric films.

Figure 2 also indicates that stoichiometry affects the bias at which Q begins to roll off due to leakage. For the e-beam contacts, this occurs at roughly the same field (−0.15 MV/cm) for all stoichiometry ratios except the very A-site-rich film, which can be biased to much higher voltages. For the sputtered contacts, a higher flux ratio correlates with lower achievable fields in Fig. 2(b), though device-to-device variations made it difficult to confirm this.

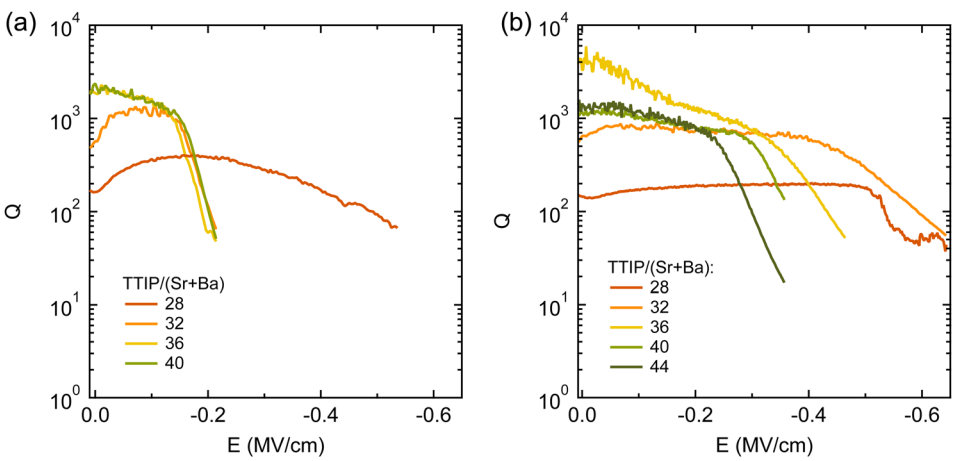

FIG. 2. Measured Q as a function of applied field for (a) e-beam contacts and (b) sputtered contacts. Negative field is plotted since application of bias in this direction probes the breakdown from injection by the top interface. While the zero-field Q is highest for stoichiometric samples (36, 40), samples with A-rich films can be biased further.

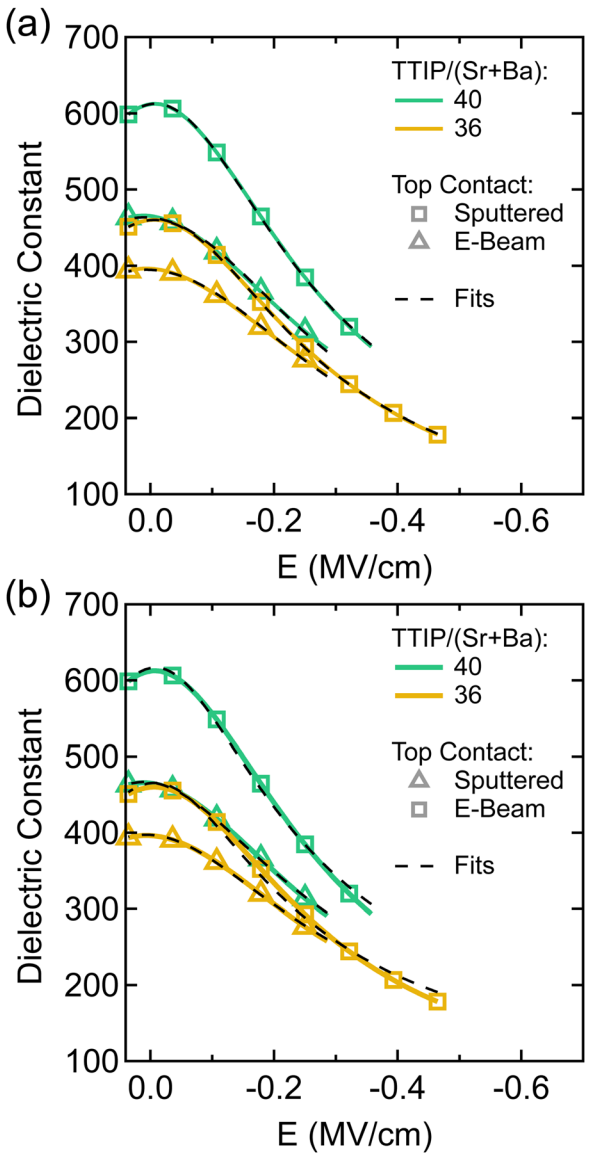

FIG. 3. Tunability measured in the apparent dielectric constant for devices with stoichiometric BST. Solid lines indicate measured data, while dotted lines show fits to (a) Eqs. (1) and (2) and (b) Eq. (3). Samples with sputter-deposited Pt top contacts show an apparent higher permittivity and tunability.

Figure 3 shows the (apparent) dielectric permittivity extracted from the device capacitance as a function of applied field. The same BST sample was split to undergo two different top contact processes. To correctly describe the device tunability and to compare the effects of the two electrodes, both the tunable dielectric constant of the BST film and any series-connected interfacial layers need to be taken into account. The interfacial capacitance reduces the overall capacitance and the voltage dropped over the tunable layer, V_B, which is described as follows:

$$V_B = E_B \times (t - t_i) = V_{App} \times \frac{\frac{\epsilon_i}{t_i}}{\frac{\epsilon_i}{t_i} + \frac{\epsilon_B(E_B)}{t - t_i}}, \quad (1)$$

where E_B is the field in the BST, $\epsilon_B(E_B)$ is field-dependent dielectric constant of the BST, V_{App} is the applied bias, and ϵ_i and t_i are the interfacial permittivity and thickness, respectively. The field dependence of the BST permittivity, $\epsilon_B(E)$, can be described by an empirical relation[23]

$$\epsilon_B(E) = \frac{b}{\sqrt{a + E^2}}. \quad (2)$$

Here, $\epsilon_B(0)$, the dielectric constant at zero bias, is $\frac{b}{\sqrt{a}}$ and b and a are temperature-dependent parameters. It has been noted that Eq. (2) has a functional form similar to the thermodynamic derivation (see below) under the Johnson approximation, which assumes a small polarization.[24] From Eq. (1), we see that when the interfacial capacitance term is very large, the device will behave like the model in Eq. (2).

For BST films of a given stoichiometry that differ only by the method used to deposit the electrodes, the parameters $\epsilon_B(0)$ and b, which is a measure of the tunability, should be identical. To fit the data shown in Fig. 3(a) to Eq. (1), $\epsilon_B(0)$ was constrained to be the same for both electrodes while b was allowed to vary. The latter was necessary because a poor fit for the sample with a flux ratio of 40 was obtained if b was constrained as well. The results are shown in Table I. The variation in b is fairly small (especially for the flux ratio of 36) but significant enough to affect the quality of the fits. The interfacial capacitance (ϵ_i/t_i) is enhanced by a factor of two to four for the sputtered contacts for the different stoichiometries. This can be explained with the removal of the low-permittivity interfacial layers by the high temperature cleaning and sputter process.[14] The device tunability, $n = C(0)/C(E)$ where $E = -0.25$ MV/cm of each device is also shown in Table I. Sputtered contacts yield higher device tunabilities than e-beam contacts at the same field, which is explained by the enhancement of the interfacial capacitance for the sputtered contact. The interface capacitance of the sputtered contacts is lower than previously reported Pt contacts on atomically smooth $SrTiO_3$ single crystals that were prepared similarly. This may be associated with other characteristics of the top interface. For example, while containing atomically stepped regions, surfaces of BST grown on Pt also show features on a larger length scale that increase the overall roughness (supplementary material). In addition to the interfacial capacitance, Table I also reveals differences in the bulk BST properties. In particular, $\epsilon_B(0)$ and b are different for the two flux ratios, even though both are within the stoichiometric growth window. We note that these two

TABLE I. Extracted fit parameters and interfacial capacitances for the curves shown in Fig. 3. Also shown is the measured device tunability at −0.25 MV/cm.

	TTIP/(Sr + Ba) = 36		TTIP/(Sr + Ba) = 40	
	Sputtered	E-beam	Sputtered	E-beam
n	1.57	1.43	1.59	1.48
Fit parameter: Eqs. (1) and (2)				
$\varepsilon_B(0)$	575		692	
b (MV/cm)	87.3	89.7	116.0	99.7
ϵ_i/t_i (nm^{-1})	8.2	4.5	19.2	5.0
E_0 (MV/cm)	−0.007	0.007	−0.008	0.010
Fit parameter: Eq. (3)				
$\varepsilon_{B,app}(0)$	466	397	617	467
E_2 (MV/cm)	0.343	0.458	0.345	0.433

parameters are not independent of each other. The reasons for the differences require further investigation, but they are also reflected in differences in Q and breakdown field, at least for the sputtered electrodes. The fits also revealed small offsets (E_0) to the maximum of the C-V curve. The sign of the offset appears related to the top contact deposition method—with a small positive offset for e-beam contacts and a small negative offset for sputtered contacts. This was also observed for the other flux ratios not shown with the exception of 28.

An alternative relation to describe the nonlinear dielectric permittivity can be derived from Landau-Ginzburg-Devonshire theory[25]

$$\epsilon_B(E) = \frac{\epsilon_{B,app}(0)}{2 \times \cosh\left[\frac{2}{3}\sinh^{-1}\left(\frac{2E}{E_2}\right)\right] - 1}, \tag{3}$$

where E_2 is the field at which $\epsilon_B(E_2) = \frac{1}{2}\epsilon_{B,app}(0)$. In Eq. (3) the effects of the interfacial capacitance are contained in $\epsilon_{B,app}(0)$ and E_2.[25] Thus, the interfacial capacitance cannot be explicitly extracted. Fits to Eq. (3) are shown in Fig. 3(b), and it can be seen that they describe the data somewhat less completely than Eq. (2). Fit values for Eq. (3) are also shown in Table I.

In conclusion, the results show that BST stoichiometry is a key factor in achieving high Q and high permittivities. Within the limits of Q measurements by an impedance analyzer, extended defects, which these films certainly contain (see AFM images in the (supplementary material)), appear to be less detrimental. Furthermore, removing interfacial parasitic layers using high temperature processes to deposit the top electrode improves the device tunability. Slightly A-rich films can, however, be biased to higher fields. Extracting the interfacial capacitance and BST dielectric properties from CV measurements revealed differences in the extracted parameters for films grown under slightly different conditions, further indicating the great sensitivity of the dielectric properties to small variations in stoichiometry.

See supplementary material for RHEED patterns acquired after growth of the BST films and atomic force microscopy images of their surfaces.

The authors thank Bob York and Cedric Meyers for discussions. The work was supported by the Army Research Office (Grant No. W911NF-14-1-0335). The authors also thank Northrop Grumman for support. This work made use of the UCSB MRL facilities, which are supported by the MRSEC Program of the NSF under Award No. DMR 1121053, and the UCSB nanofabrication facility. C.R.F. also acknowledges funding by the Department of Defense (DoD) through the National Defense Science & Engineering Graduate Fellowship (NDSEG) Program.

[1]R. A. York, in *Multifunctional Adaptive Microwave Circuits and Systems*, edited by M. Steer and W. D. Palmer (SciTech Publishing, 2009).
[2]A. K. Tagantsev, V. O. Sherman, K. F. Astafiev, J. Venkatesh, and N. Setter, J. Electroceram. **11**, 5 (2003).
[3]G. Subramanyam, M. W. Cole, N. X. Sun, T. S. Kalkur, N. M. Sbrockey, G. S. Tompa, X. M. Guo, C. L. Chen, S. P. Alpay, G. A. Rossetti *et al.*, J. Appl. Phys. **114**, 191301 (2013).
[4]N. M. Sbrockey, T. S. Kalkur, A. Mansour, H. Khassaf, H. Yu, M. Aindow, S. P. Alpay, and G. S. Tompa, Appl. Phys. Lett. **109**, 052902 (2016).
[5]G. N. Saddik, J. Son, S. Stemmer, and R. A. York, J. Appl. Phys. **109**, 091606 (2011).
[6]T. J. Jackson and I. P. Jones, J. Mater. Sci. **44**, 5288 (2009).
[7]E. Mikheev, A. P. Kajdos, A. J. Hauser, and S. Stemmer, Appl. Phys. Lett. **101**, 252906 (2012).
[8]B. Jalan, P. Moetakef, and S. Stemmer, Appl. Phys. Lett. **95**, 032906 (2009).
[9]A. P. Kajdos and S. Stemmer, Appl. Phys. Lett. **105**, 191901 (2014).
[10]D. J. Keeble, B. Jalan, L. Ravelli, W. Egger, G. Kanda, and S. Stemmer, Appl. Phys. Lett. **99**, 232905 (2011).
[11]T. A. Cain, A. P. Kajdos, and S. Stemmer, Appl. Phys. Lett. **102**, 182101 (2013).
[12]S. K. Streiffer, C. Basceri, C. B. Parker, S. E. Lash, and A. I. Kingon, J. Appl. Phys. **86**, 4565 (1999).
[13]B. Jalan, J. Cagnon, T. E. Mates, and S. Stemmer, J. Vac. Sci. Technol., A **27**, 1365 (2009).
[14]E. Mikheev, B. D. Hoskins, D. B. Strukov, and S. Stemmer, Nat. Commun. **5**, 3990 (2014).
[15]H. Rohdin, N. Moll, A. M. Bratkovsky, and C. Y. Su, Phys. Rev. B **59**, 13102 (1999).
[16]J. Son, J. Cagnon, and S. Stemmer, J. Appl. Phys. **106**, 043525 (2009).
[17]B. Jalan, R. Engel-Herbert, N. J. Wright, and S. Stemmer, J. Vac. Sci. Technol., A **27**, 461 (2009).
[18]T. Ohnishi, K. Shibuya, T. Yamamoto, and M. Lippmaa, J. Appl. Phys. **103**, 103703 (2008).
[19]Y. Matsubara, K. S. Takahashi, Y. Tokura, and M. Kawasaki, Appl. Phys. Express **7**, 125502 (2014).
[20]B. Bauer and W. Richter, *Optical Characterization of Epitaxial Semiconductor Layers* (Springer, Berlin, 1996).
[21]N. K. Pervez, J. Park, J. W. Lu, S. Stemmer, and R. A. York, Integr. Ferroelectr. **77**, 87 (2005).
[22]K. F. Astafiev, A. K. Tagantsev, and N. Setter, J. Appl. Phys. **97**, 014106 (2005).
[23]S. Suzuki, T. Yamamoto, H. Suzuki, K. Kawaguchi, K. Takahashi, and Y. Yoshisato, J. Appl. Phys. **81**, 6830 (1997).
[24]L-P. Curecheriu, Processing and Application of Ceramics **1**, 23 (2007).
[25]D. R. Chase, L. Y. Chen, and R. A. York, IEEE Trans. Microwave Theory Tech. **53**, 3215 (2005).